Self-assembly of patchy particles into polymer chains: A parameter-free comparison between Wertheim theory and Monte Carlo simulation

Francesco Sciortino
Dipartimento di Fisica and INFM-CNR-SOFT, Università di Roma La Sapienza, Piazzale Aldo Moro 2, 00185 Roma, Italy

Emanuela Bianchi
Dipartimento di Fisica and INFM-CNR-SMC, Università di Roma La Sapienza, Piazzale Aldo Moro 2, 00185 Roma, Italy

Jack F. Douglas
Polymers Division, National Institutes of Standards and Technology, Gaithersburg, Maryland 20899

Piero Tartaglia
Dipartimento di Fisica and INFM-CNR-SMC, Università di Roma La Sapienza, Piazzale Aldo Moro 2, 00185 Roma, Italy

The authors numerically study a simple fluid composed of particles having a hard-core repulsion, complemented by two short-ranged attractive (sticky) spots at the particle poles, which provides a simple model for equilibrium polymerization of linear chains. The simplicity of the model allows for a close comparison, with no fitting parameters, between simulations and theoretical predictions based on the Wertheim perturbation theory. This comparison offers a unique framework for the analytic prediction of the properties of self-assembling particle systems in terms of molecular parameters and liquid state correlation functions. The Wertheim theory has not been previously subjected to stringent tests against simulation data for ordering across the polymerization transition. The authors numerically determine many of the thermodynamic properties governing this basic form of self-assembly (energy per particle, order parameter or average fraction of particles in the associated state, average chain length, chain length distribution, average end-to-end distance of the chains, and the static structure factor) and find that predictions of the Wertheim theory accord remarkably well with the simulation results. © *2007 American Institute of Physics*. [DOI: 10.1063/1.2730797]

I. INTRODUCTION

Recently, there has been great interest in exploiting self-assembly to create functional nanostructures in manufacturing, and this challenge has stimulated a great deal of experimental and theoretical activities.[1–13] Self-assembly has been considered for over 50 years to be central to understanding structure formation in living systems, and thus, modeling and measurements of naturally occurring self-assembling systems has long been pursued in the biological sciences.[12] Even the term self-assembly derives from an appreciation of the capacity of viruses to spontaneously reconstitute themselves from their molecular components,[14,15] much as in the familiar example of micelle formation by block copolymers, lipids, and other surfactant molecules exhibiting amphiphilic interactions. The diversity and morphological and functional complexity of viruses, as well as the vast number of self-assembly biological processes in living systems, point to the potential of this type of organizational processes for manufacturing new materials. While the potential of self-assembly as a manufacturing strategy is clear, our understanding of how this process actually works is still incomplete and many of the basic principles governing this type of organization are unclear. An evolutionary (trial and error) approach to this

problem is not very efficient for manufacturing. There is evidently a need for developing a first principles understanding of this phenomenon where no free parameters are involved in the theoretical description in order to elucidate the fundamental mechanisms governing self-assembly and the observables required to characterize the interactions governing thermodynamic self-assembly transitions, at least for simple model systems that can be subjected to high resolution investigation.

As a starting point for this type of fundamental investigation of self-assembly, we consider the problem of the equilibrium polymerization of linear polymer chains,[16–18] which is arguably the simplest variety of thermally reversible particle assembly into extended objects (polymers in the case of our molecular model). To investigate this problem analytically, we exploit the Wertheim thermodynamic perturbation theory (W-TPT), which offers a systematic molecularly based framework for calculating the thermodynamic properties of self-assembling systems, although this theory has rarely before been applied to this purpose.[19] The Wertheim theory has been previously considered to better understand properties of associating fluids. A sticky sphere model, similar to the one we consider below, has been studied to determine how particle association affects critical properties in

competition with fluid phase separation (critical temperature and composition, binodals, critical compressibility factor, etc.[20–22]). Similar models have also been considered to determine the effect of association on nucleation[23] and model antigen-antibody bonding.[24] In contrast, we are concerned here with the thermodynamic transition that accompanies the self-assembly of the particles into organized structures due to their anisotropic interactions.

The Wertheim theory is certainly not a unique theory of the thermodynamics of self-assembling particle systems. Models of equilibrium polymerization of linear, branched, and compact structures have all been introduced based on the concept of an association equilibrium being established between the assembling particles, and a comparison of this type of theory to simulation has led to remarkably good agreement.[12,25–31] Up to the present time, however, it has been necessary to adjust the entropy of association parameter in this class of theories, so that the modeling is not really fully predictive (see discussion in Sec. III where this quantity is explicitly determined from the Wertheim theory). The unique aspect of W-TPT is that all the interaction parameters of this theory can be directly calculated from the knowledge of the intermolecular potential and from a standard liquid state correlation functions, so that the theory is fully predictive. It has also been shown that W-TPT is formally equivalent to association-equilibrium models of self-assembly.[19] Hence, the Wertheim theory also offers the prospect of being able to improve the predictive character of these other theories if the theory itself can be validated as being reliable. The Wertheim theory is based on a formal perturbation theory,[32–34] and there are naturally questions about the accuracy that can be expected from this theory.

The present paper considers a stringent test of Wertheim theory as a model of the thermodynamics of self-assembly by comparing precise numerical Monte Carlo (MC) data for the thermodynamic properties of our model associating fluid to the analytic predictions of the Wertheim theory where there are no free parameters in the comparison. Notably, many of the properties that we consider have never been considered before in the Wertheim theory.

II. TWO PATCHY SITES PARTICLE MODEL

We focus on a system of hard-sphere (HS) particles (of diameter σ, the unit of length) whose surface is decorated by $M=2$ identical sites oppositely located (see Fig. 1).

The interaction $V(1,2)$ between particles 1 and 2 is

$$V(1,2) = V_{HS}(\mathbf{r}_{12}) + \sum_{i=1,2} \sum_{j=1,2} V_W(\mathbf{r}_{12}^{ij}), \qquad (1)$$

where V_{HS} is the hard-sphere potential, $V_W(x)$ is a square-well interaction (of depth $-u_0$ for $x \lesssim \delta$, 0 otherwise), and $\mathbf{r}_{12}$ and $\mathbf{r}_{12}^{ij}$ are, respectively, the vectors joining the particle-particle centers and the site-site (on different particles) locations. Temperature is measured in units of the potential depth (i.e., Boltzmann constant $k_B=1$). Geometric considerations for a three touching spheres configuration show that the choice of well width $\delta=0.5(\sqrt{5-2\sqrt{3}}-1)\sigma \approx 0.119\sigma$ guarantees that each site is engaged at most in one bond. Hence,
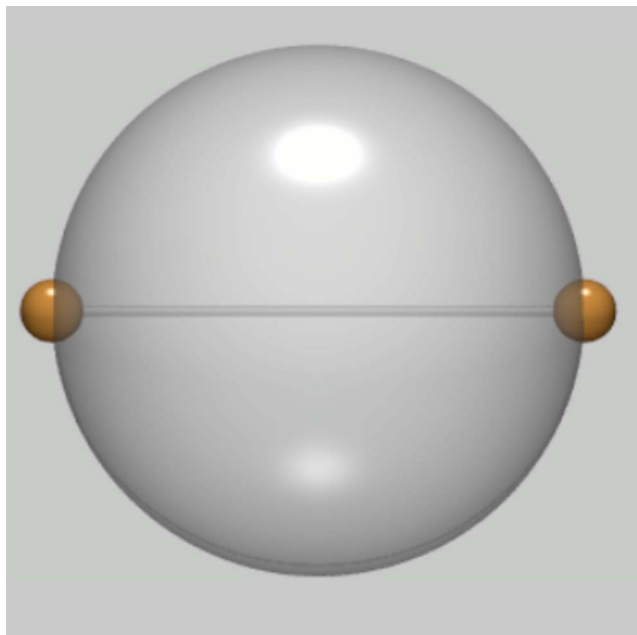

FIG. 1. (Color online) Pictorial representation of the model studied. Particles are modeled as hard-core spheres (gray large sphere of diameter σ), decorated by two sites located on the surface along a diameter (centers of the small gold spheres of diameter 2δ). The volume of the gold sphere outside the gray large sphere is the bonding volume. When the site of another particle is located within the bonding volume, the pair interaction energy is taken to be equal to $-u_0$.

each particle can form only up to two bonds, and, correspondingly, the lowest energy per particle ("sticking energy") is $-u_0$.

The choice of a simple square-well interaction model to describe the association process between different particles is particularly convenient from a theoretical point of view. It allows for a clear definition of bonding and a clear separation of the bond free energy in energetic and entropic contributions, being unambiguously related to the depth of the well and to the bonding volume, respectively.

III. WERTHEIM THEORY

The first-order Wertheim thermodynamic perturbation theory[32–35] provides an expression for the free energy of associating liquids. The Helmholtz free energy is written as a sum of the HS reference free energy A_{HS} plus a bond contribution A_{bond}, which is derived by a summation over certain classes of relevant graphs in the Mayer expansion.[35] In the sum, closed loops graphs are neglected. The fundamental assumption of W-TPT is that the conditions of steric incompatibilities are satisfied: (i) no site can be engaged in more than one bond and (ii) no pair of particles can be double bonded. These steric incompatibilities are satisfied in the present model, thanks to the location of the two sites and the chosen δ value. In the formulation of Ref. 36, for particles with two identical bonding sites,

$$\frac{\beta A_{bond}}{N} = 2 \ln X - X + 1. \qquad (2)$$

Here, $\beta=1/k_BT$ and X is the fraction of sites that are not bonded. X is calculated from the mass-action equation

$$X = \frac{1}{1 + 2\rho X \Delta}, \tag{3}$$

where $\rho = N/V$ is the particle number density and Δ is defined by

$$\Delta = 4\pi \int g_{HS}(r_{12}) \langle f(12) \rangle_{\omega_1, \omega_2} r_{12}^2 \, dr_{12}. \tag{4}$$

Here, $g_{HS}(12)$ is the reference HS fluid pair correlation function, the Mayer f function is $f(12) = \exp(-V_W(\mathbf{r}_{12}^{ij})/k_B T) - 1$, and $\langle f(12) \rangle_{\omega_1, \omega_2}$ represents an angle average over all orientations of particles 1 and 2 at a fixed relative distance r_{12}. Since all bonding sites are identical (same depth and width of the square-well interaction), Δ refers to a single site-site interaction. The number of attractive sites on each particle is encoded in the factor 2 in front of Δ in Eq. (3). In the W-TPT, the resulting free energy is insensitive to the location of the attractive sites, i.e., to the bonding geometry of the particle. Note that the angle averaged Mayer f function coincides with the bonding interaction contribution to the virial coefficient. At low T (i.e., $\beta u_0 \gg 1$) the hard-core contribution to the virial becomes negligible as compared to the bonding component. In this limit, it is also possible to assume $\exp(\beta u_0) - 1 \approx \exp(\beta u_0)$, so that the averaged Mayer f function can be approximated with the virial as well as with the integral of the Boltzmann factor over the bond volume.[38]

For a site-site square-well interaction, the Mayer function can be calculated as[37]

$$\langle f(12) \rangle_{\omega_1, \omega_2} = [\exp(\beta u_0) - 1] S(r), \tag{5}$$

where

$$S(r) = \frac{(\delta + \sigma - r)^2 (2\delta - \sigma + r)}{6\sigma^2 r} \tag{6}$$

is the fraction of solid angle available to bonding when two particles are located at relative center-to-center distance r. Thus, the evaluation of Δ requires only an expression for $g_{HS}(r_{12})$ in the range where bonding occurs ($\sigma < r < \sigma + \delta$). We have used the linear approximation[39]

$$g_{HS}(r) = \frac{1 - 0.5\phi}{(1-\phi)^3} - \frac{9}{2} \frac{\phi(1+\phi)}{(1-\phi)^3} \left[\frac{r-\sigma}{\sigma} \right] \tag{7}$$

[where $\phi = (\pi/6)\sigma^3 \rho$], which provides the correct Carnahan-Starling[40] value at contact. This gives

$$\Delta = \frac{V_b(e^{\beta u_0} - 1)}{(1-\phi)^3} \times \left[1 - \frac{5}{2} \frac{(3\sigma^2 + 8\delta\sigma + 3\delta^2)}{\sigma(15\sigma + 4\delta)} \phi \right.$$
$$\left. - \frac{3}{2} \frac{(12\delta\sigma + 5\delta^2)}{\sigma(15\sigma + 4\delta)} \phi^2 \right], \tag{8}$$

where we have defined the spherically averaged bonding volume $V_b \equiv 4\pi \int_\sigma^{\sigma+\delta} S(r) r^2 dr = \pi\delta^4(15\sigma + 4\delta)/30\sigma^2$. For the specific value of δ studied here, $V_b = 0.000\,332\,285\sigma^3$. At low ϕ, $g_{HS}(r)$ tends to the ideal gas limit value $g_{HS}(r) \approx 1$. In this limit

$$\Delta = V_b(e^{\beta u_0} - 1). \tag{9}$$

Equation (3) can be easily solved, providing the T and ρ dependence of X as

$$X = \frac{2}{1 + \sqrt{1 + 8\rho\Delta}}, \tag{10}$$

which has a low-T limit $X \approx \sqrt{2\rho\Delta}$.

In the more transparent chemical equilibrium form, Eq. (10) can be written as

$$\frac{1-X}{X^2} = 2\rho\Delta = \rho K_b. \tag{11}$$

The last expression shows that, within the Wertheim theory, bonding can be seen as a chemical reaction between two unreacted sites forming a bonded pair. In this language the quantity $K_b \equiv 2\Delta$ plays the role of equilibrium constant (in unit of inverse concentration). Writing $\rho K_b = \exp\{-\beta(\Delta U_b - T\Delta S_b)\}$ (introducing the energy and entropy change in the bond process), it is possible to provide precise expressions for ΔU_b and ΔS_b within the Wertheim theory. Specifically, when $e^{\beta u_0} \gg 1$ (a very minor approximation since aggregation requires $T \ll u_0$ to be effective), it is possible to identify

$$\Delta U_b = -u_0, \tag{12}$$

$$\Delta S_b = \ln\left[8\pi\rho \int_\sigma^{\sigma+\delta} g_{HS}(r) S(r) r^2 dr \right] \tag{13}$$

(note that ΔS_b is in dimensionless entropy units since Boltzmann constant is taken equal to 1). If $g_{HS} \approx 1$, $\Delta S_b = \ln(2NV_b/V)$. Hence, the change in energy is given by the bond energy, while the change in entropy is essentially provided by the logarithm of the ratio between the bonding volume and the volume per site ($V/2N$).

IV. CLUSTER SIZE DISTRIBUTIONS AND ASSOCIATION PROPERTIES

It is interesting to discuss the prediction of the Wertheim theory in terms of clusters of physically bonded particles.[41,42] In the case of square-well interactions (different from the case of a continuous potential) we can define a bond between two particles unambiguously. Evidently, when there is a bond, the interaction energy equals $-u_0$.

To make the discussion more transparent, we can define $p_b \equiv 1 - X$ as the probability that an arbitrary site is bonded. It is thus easy to convince oneself that the number density of monomers is $\rho_1 = \rho(1 - p_b)^2 = \rho X^2$ since both sites must be unbonded.[19] Similarly, a chain of l particles has a number density ρ_l equal to

$$\rho_l = \rho(1 - p_b)^2 p_b^{(l-1)} = \rho X^2 (1 - X)^{(l-1)} \tag{14}$$

since one site of the first and one of the last particle in the chain must be unbonded and $l - 1$ bonds link the l particles.

Once the cluster size distribution of chains is known, it is possible to calculate the average chain length L as the ratio between the total number density and the number density of chains in the system, (i.e., as the ratio between the first $\langle l^1 \rangle$ and the zero $\langle l^0 \rangle$ moments of the ρ_l distribution)
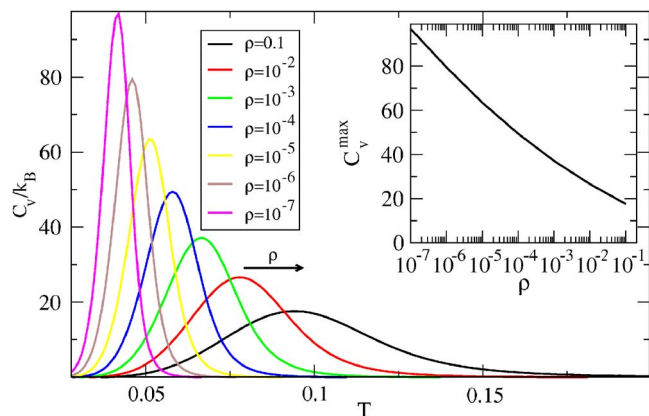
FIG. 2. (Color online) W-TPT predictions for the T dependence of the specific heat C_V for different values of densities ρ [Eq. (19)]. The inset shows the value of the specific heat at the maximum $C_V^{\max}$.

$$L \equiv \frac{\sum_{l=1}^{\infty} l\rho_l}{\sum_l \rho_l} = \frac{1}{X}, \qquad (15)$$

where we have substituted, by summing the geometric series over all chain lengths, $\sum_{l=1}^{\infty} l\rho_l = \rho$ and $\sum_{l=1}^{\infty} \rho_l = \rho X$. Thus, using Eq. (10),

$$L = \frac{1 + \sqrt{1 + 8\rho\Delta}}{2}. \qquad (16)$$

At low T, $L \approx \sqrt{2\rho\Delta}$ and hence L grows in density as $\sqrt{\rho}$ (if the density dependence of Δ can be neglected[43]) and in T as $L \sim \exp(\beta u_0/2)$.

The potential energy of the system coincides with the number of bonds (times $-u_0$). Hence, the energy per particle E/N is

$$E/N = -u_0 \frac{\sum_{l=1}^{\infty} (l-1)\rho_l}{\sum_{l=1}^{\infty} l\rho_l} = -u_0(1-X) = -u_0 p_b. \qquad (17)$$

The energy approaches its ground state value ($E_{gs}/N = -u_0$) as

$$\frac{E - E_{gs}}{N} = u_0 X \approx u_0 (2\rho\Delta)^{-1/2}, \qquad (18)$$

i.e., with an Arrhenius law with activation energy $u_0/2$ in the low-T limit, a signature of independent bonding sites.[44–46]

From Eq. (17) it is possible to calculate the (constant volume) specific heat C_V as

$$C_V = C \frac{X^2 e^{\beta u_0} \rho}{\sqrt{1 + 8\rho\Delta} T^2}, \qquad (19)$$

where $C = 8\pi u_0^2 \int_\sigma^{\sigma+\delta} g_{HS}(r) S(r) r^2 dr$. In the low T and ρ regimes, the specific heat becomes $C_V \approx X/2T^2$. At each ρ, the specific heat shows a maximum at a finite T (see Fig. 2), which defines a line of specific heat extrema in the T-ρ plane. The location of the maximum in the specific heat has been utilized to estimate the polymerization temperature $T_{C_V^{\max}}$.[16–18,26,47,48]

Within the theory, it is also possible to evaluate the extent of polymerization Φ, defined as the fraction of particles connected in chains (chain length larger than 1), i.e.,
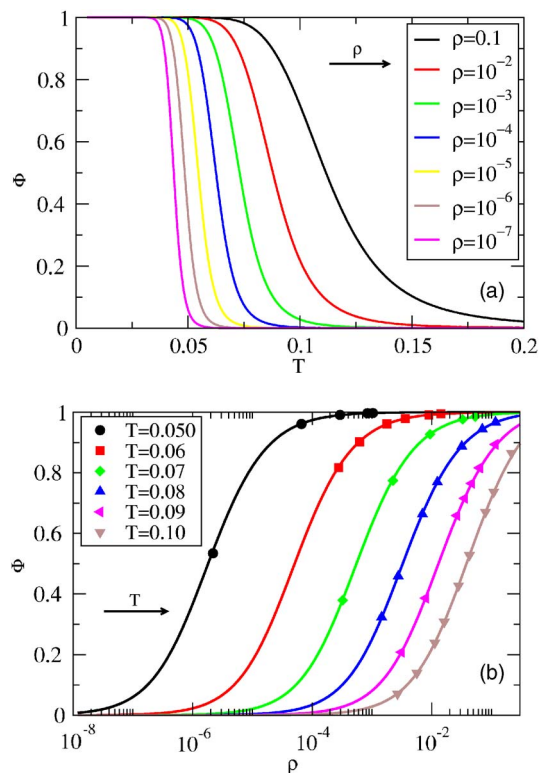

FIG. 3. (Color online) Extent of polymerization Φ vs temperature T (a) and density ρ (b). Symbols are GC simulation data.

$$\Phi = \frac{\sum_{l=2}^{\infty} l\rho_l}{\sum_{l=1}^{\infty} l\rho_l} = 1 - \frac{\rho_1}{\rho} = 1 - X^2, \qquad (20)$$

where we have used Eq. (14). Φ plays the role of order parameter for the polymerization transition. The density and temperature dependence of Φ are shown in Fig. 3. The crossover from the monomeric state at high T ($\Phi \approx 0$) to the polymeric thermodynamic state at low T ($\Phi \approx 1$) takes place in a progressively smaller T window on decreasing ρ.

For each ρ, a transition temperature T_Φ can be defined as the *inflection point* of Φ as a function of T.[16–18,47,48] The locus $T_\Phi(\rho)$ provides an estimate of the polymerization line in the phase diagram. The location of the inflection point of the energy E and of Φ are different since $dE/dT \sim dX/dT$ [Eq. (17)], while $d\Phi/dT \sim -XdX/dT$ [Eq. (20)]. In other models of equilibrium polymerization, incorporating thermal activation or chemical initiation, T_Φ and $T_{C_V^{\max}}$ coincide.[47,49]

Another estimate of the transition line of this rounded thermodynamic transition can be defined as the locus in the T-ρ plane at which $\Phi = 0.5$; i.e., half of the particles are in chain form (the analog of the critical micelle concentration[50]), i.e., $\rho_1(T_{1/2}, \rho) = \rho/2$. The corresponding temperature $T_{1/2}$ is then given by the solution of the equation $X = \sqrt{0.5}$ or, equivalently,

$$\rho\Delta = 1 - \sqrt{0.5}. \qquad (21)$$

In the present model, the $\Phi = 0.5$ locus is a line at constant p_b, corresponding to a constant value of the product $\rho[\exp(\beta u_0) - 1]$.

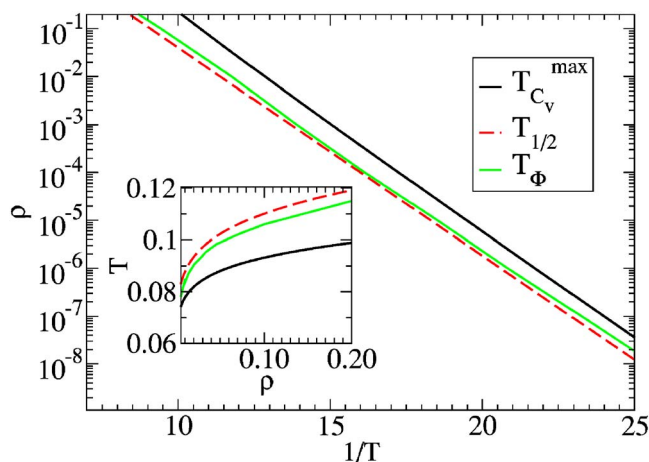To provide a global view of the polymerization transition, we show in Fig. 4 the Wertheim theory predictions for

FIG. 4. (Color online) Specific heat maxima and polymerization transition lines, as predicted by the Wertheim theory, in the T-ρ plane. The inset shows the linear scale. Observe the similarity of the data in Figs. 2–4 to that of Figs. 4–6 in Ref. 29 corresponding to equilibrium polymerization in the Stockmayer fluid, a Lennard-Jones particle with a superimposed point dipole.

the specific heat maximum and polymerization transition lines. Curves become progressively more and more similar on cooling. As clearly shown by the simple expression for $T_{1/2}$ [Eq. (21)], the quantity $\rho\Delta$ is constant, which implies that $\ln \rho \sim 1/T$. This behavior is also approximatively found for the loci defined by the inflection point of Φ and E, as shown in Fig. 4.

It is interesting to estimate the value of the average degree of polymerization L along the polymerization transition line. This information helps in estimating the polymerization transition itself, but it is also relevant for the recently proposed analogies between polymerizing systems and glass-forming liquids.[51] As shown in Fig. 5, the transition takes place for $L \approx 2$, consistent with previous findings (compare with the inset of Fig. 7 in Ref. 27 for the Stockmayer fluid). The fact that $L \approx 2$ near T_ϕ provides a way to estimate the polymerization transition temperature when experimental (or numerical) data are noisy.[30]

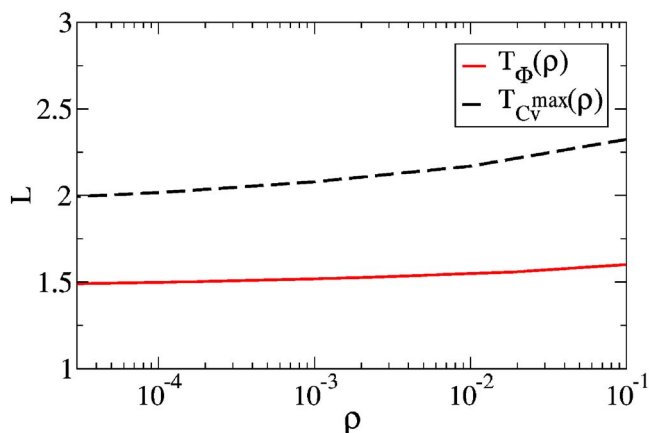A final relevant consideration concerns the expression

FIG. 5. (Color online) Value of the average chain length along the polymerization lines $T_\Phi(\rho)$ (solid line) and $T_{C_V}^{max}(\rho)$ (dotted line), according to the Wertheim theory.

for the bonding free energy. Under the assumption of an ideal state of chains, the system free energy A can be written as[28]

$$\beta A/V = \sum_{l=1}^{\infty} \rho_l [\ln \rho_l - 1 + (l-1)\ln K_b], \quad (22)$$

which accounts for the translational entropy of the clusters as well as for the bond free energy $\ln K_b$, which is assumed to be linear in the number of bonds. At high T only monomers are present, $\rho_l = \rho \delta_{l1}$, and hence $\beta A/V = \rho[\ln \rho - 1]$. The bonding part of the free energy βA_{bond} can thus be evaluated as the difference of βA and the corresponding high-T limit, i.e.,

$$\beta A_{bond}/V = \sum_{l=1}^{\infty} \rho_l [\ln \rho_l - 1 + (l-1)\ln K_b] - \rho[\ln \rho - 1]. \quad (23)$$

Inserting the Wertheim cluster size distribution [Eq. (14)], summing over all cluster size and using the definition $K_b \equiv 2\Delta$ [Eq. (11)], one exactly recovers the Wertheim bonding free energy [Eq. (2)]. The Wertheim theory can thus be considered as a mean-field theory of chain associations, with the hard-sphere free energy as its high-T limit. Differently from other mean-field approaches,[28,43,47,52] the theory provides a well-defined prescription for calculating the equilibrium constant as well as the energy and the entropy of assembling, which partially account for the structure of the reference hard-sphere fluid via the $g_{HS}(r)$ contribution in K_b. It is this special feature that makes the theory fully predictive.

V. MONTE CARLO SIMULATION

We have performed numerical simulations of the model in the grand-canonical (GC) ensemble[53] for several values of T and of activities to evaluate the structural properties of the system as a function of density and temperature. We have performed two types of grand-canonical simulations: particle and chain insertion/removal.

The first method (particle) is a classical GC MC simulation where monomers are individually added to or eliminated from the system with insertion and removal probabilities given by

$$P_{insertion} = \min\left(1, \frac{zV}{N+1}e^{-\beta\Delta E}\right), \quad (24)$$

$$P_{removal} = \min\left(1, \frac{N}{V}\frac{e^{\beta\Delta E}}{z}\right), \quad (25)$$

where N is the number of monomers, ΔE is the change in the system energy upon insertion (or removal), and z is the chosen activity. We have simulated for about 2×10^6 MC steps, where a MC step has been defined as 50 000 attempts to move a particle and 100 attempts to insert or delete a particle. A move is defined as a displacement in each direction of a random quantity distributed uniformly between $\pm 0.05\sigma$ and a rotation around a random axis of a random angle distributed uniformly between ± 0.1 radiant. The box size has been fixed to 50σ. With this type of simulations we have

studied three temperatures ($T=0.08$, 0.09, and 0.1) and several densities ranging from 0.001 up to 0.2 (corresponding to number N of particles ranging from $N \approx 1000$ to $N \approx 20\,000$).

The second method is grand-canonical simulations where we add and remove chains of particles (see, for example, Ref. 29). The insertion and removal probabilities for a chain of length l are

$$P_{\text{insertion}} = \min\left(1, \frac{z^l e^{-(l-1)\beta f_b} V}{N_i + 1} e^{-\beta \Delta E}\right), \tag{26}$$

$$P_{\text{removal}} = \min\left(1, \frac{N_l}{V} \frac{e^{\beta \Delta E}}{z^l e^{-(l-1)\beta f_b}}\right), \tag{27}$$

where N_l is the number of chains of size l, ΔE is the change in energy, and βf_b is the ln of the integral of the Boltzmann factor over the bond volume, i.e.,

$$\beta f_b = \beta u_0 - \ln[2V_b]. \tag{28}$$

The activity of a chain of l particles is thus written as $z_l = z^l e^{-(l-1)\beta f_b}$ or, equivalently, in terms of chemical potential $\mu_l = l\mu - (l-1)f_b$, where μ is the monomer chemical potential. Using the chain insertion algorithm, we have followed the system for about 10^5 MC steps, where a MC step has now been defined as 50 000 attempts to move a particle (as in the previous type) and 100 attempts to insert or delete a chain of randomly selected length. The geometry of the chain to be inserted is also randomly selected. The box size was varied from 50σ to 400σ, according to density and temperature, to guarantee that the longest chain in the system was always shorter than the box size. At the lowest T, $N \approx 50\,000$. Using chain moves, we have been able to equilibrate and study densities ranging from 10^{-6} up to 0.2 for four low temperatures ($T=0.05$, 0.055, 0.6, and 0.7) where chains of length up to 400 monomers are observed. We have also studied the same three temperatures ($T=0.08$, 0.09, and 0.1) examined with the particle insertion/removal method to compare the two MC approaches.

As a result of the long simulations performed (about three months of CPU time for each state point), resulting average quantities calculated from the MC data ($L, \Phi, E/N$) are affected by less than 3% relative error. Chain length distributions ρ_l (whose signal covers up to six orders of magnitude) are affected by an error proportional to $|\ln(\rho_l)|$ which progressively increases on decreasing ρ_l, reaching 70% at the smallest reported ρ_l values.

VI. SIMULATION RESULTS

First, we begin by showing in Fig. 6 representative particle configurations both above and below the polymerization transition temperature T_ϕ. Evidently, the particles are dispersed as a gas of monomers and as a gas of chains above and below this characteristic temperature. The low-T configuration is composed of semiflexible chains, with no rings. Indeed, the short interaction range δ introduces a significant stiffness in the chain and a persistence length extending over several monomers.

To quantify the linearity of the chains for the present model we show in Fig. 7 the chain end-to-end squared
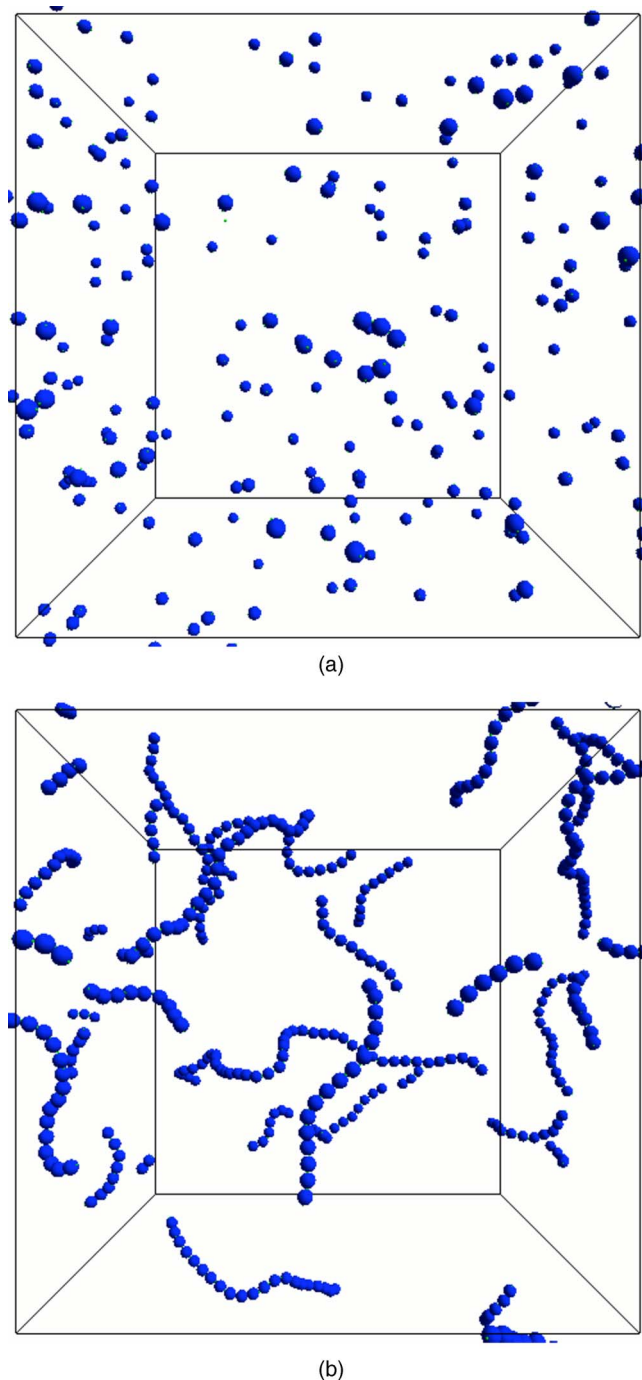

(a)

(b)

FIG. 6. (Color online) Snapshots of a fraction of the simulated system at $\rho \approx 0.0035$ and $T=0.10$ and $T=0.055$. At this density, the polymerization transition is located at $T_\Phi \approx 0.08$. The length of the shown box edge is about 30σ.

distance $\langle R_e^2 \rangle$ for isolated chains of chain length up to $l \sim O(10^3)$. Single chains are generated by progressively adding monomers to a preexisting chain in a bonding configuration, after checking the possible overlap with all preexisting monomers. Since the bond interaction is a well, all points in the bond volume have the same *a priori* probability. As shown in Fig. 7, the end-to-end chain distance scales as a power law ($\langle R_e^2 \rangle \sim l^{2\nu}$) both at small and large l values, with a crossing between two different behaviors around $l \simeq O(10)$. At small l, the chain is persistent in form and thus
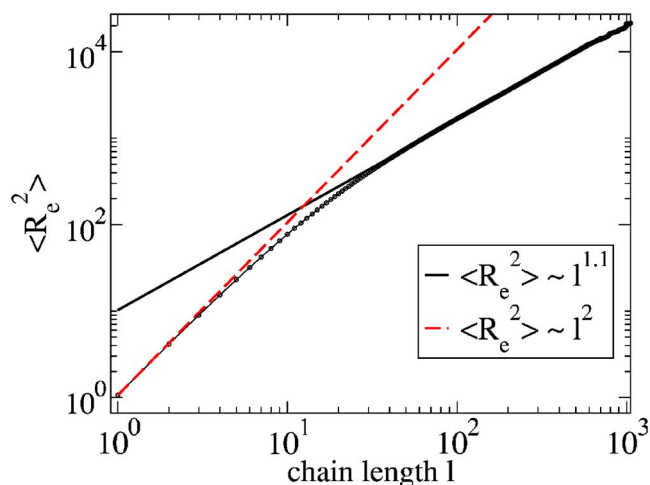
FIG. 7. (Color online) Mean squared end-to-end distance $\langle R_e^2 \rangle$ for isolated chains of length l built according to the model studied in this article.

is rodlike. For larger l, the best fit with a power law suggests an apparent exponent $2\nu \approx 1.1$, which is expected to evolve—for very long chains—toward the self-avoiding value $2\nu \approx 1.18$.[54,55] We recall that $2\nu = 6/5$ in the Flory self-consistent field prediction[56] and $2\nu = 1$ in the simple random walk model.[56]

To provide evidence that the chain GC MC simulation provides the correct sampling of the configurations (and hence that the activity of the chain of length l is correctly assigned), we compare in Fig. 8 the chain length densities ρ_l calculated with the two methods at $T=0.08$. The distributions calculated with the two different methods are identical. A similar agreement is also found at $T=0.09$ and $T=0.1$. This strengthens the possibility of using the chain MC method, which does not significantly suffer from the slow equilibration process associated with the increase of the Boltzmann factor $\exp(\beta u_0)$ on cooling. All the following data are based on chain GC-MC simulations.
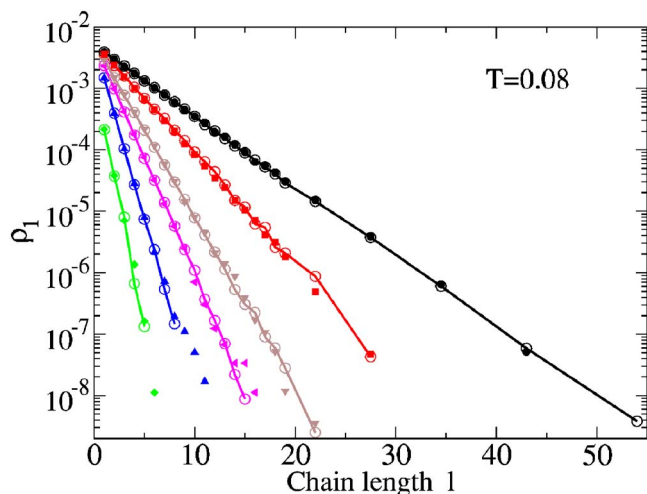

FIG. 8. (Color online) Comparison of the chain length distributions ρ_l at $T=0.08$ obtained independently with the monomer (full symbols) and chain (lines connecting open symbols) grand-canonical simulations for several values of the monomer activity z. From left to right, the activity values are 10^{-3}, 1.5×10^{-3}, 2.4×10^{-3}, 3×10^{-3}, 5×10^{-3}, and 6×10^{-3}. A similar agreement is also found at the other temperatures.
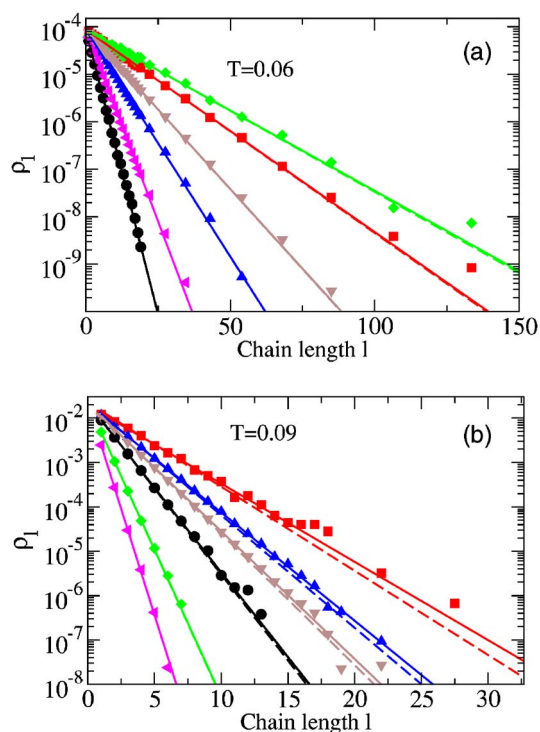

FIG. 9. (Color online) Chain length densities ρ_l for several activity values at two different temperatures, $T=0.06$ and $T=0.09$. Symbols are simulation data. Lines are Wertheim theory predictions: dashed lines assume $g_{HS}=1$ [Eq. (9) for $\triangle$], while full lines are based on the full radial dependence of g_{HS} [Eq. (8) for $\triangle$]. At the lowest T (and average densities), the ideal gas approximation is sufficient to model the Monte Carlo data.

We next compare the chain length distributions calculated using the chain MC method with the predictions of the Wertheim theory. We compare the simulation data with two different approximations: in the first one we choose the ideal gas as a reference state; i.e., we approximate the reference radial distribution function as one. In the more realistic approximation, we use the small r expansion of the hard-sphere radial distribution function [see Eq. (7)]. A comparison between simulation data and theoretical predictions (note there are no fitting parameters) is reported in Fig. 9 for two different temperatures. At low densities (sampled at low T) the approximation $g_{HS} \approx 1$ is already sufficient to properly describe ρ_l. At higher densities (sampled at higher T), the full theory is required to satisfactory predict the chain length distributions.

Figure 10(a) compares the Wertheim theory predictions for the average chain length with the corresponding simulation results. In the entire investigated ρ and T ranges, the Wertheim theory provides an accurate description of the equilibrium polymerization process. The limiting growth law in $\sqrt{\rho}$ is clearly visible at the lowest temperatures. At the highest temperatures, it is possible to access the region of larger densities ($\rho \sim 0.1$) where the presence of other chains cannot be neglected any longer and Δ becomes ρ dependent. In this limit, the growth law $L \sim \sqrt{\rho}$ is no longer obeyed.[43] As a further check on the Wertheim theory, we collapse all the L data to the universal functional form predicted by the Wertheim theory using the scaling variable $2\Delta\rho$ [Fig. 10(b)].

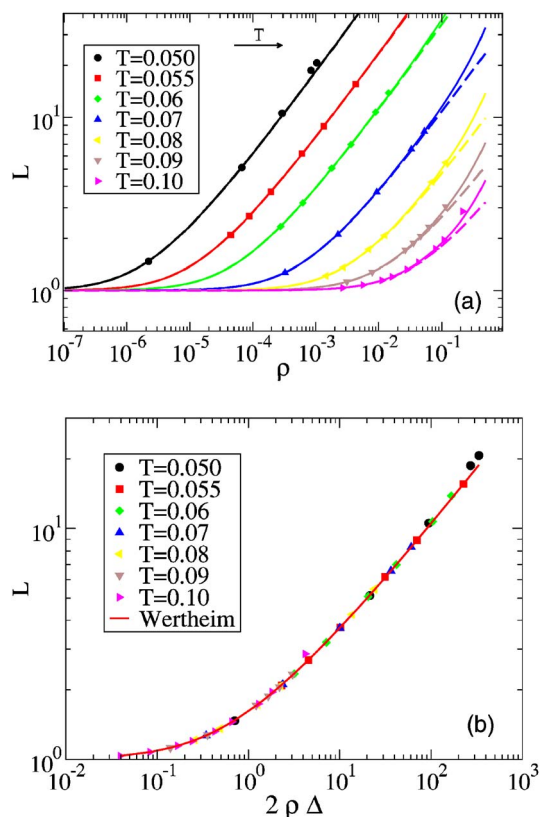As an ulterior confirmation of the predictive capabilities

FIG. 10. (Color online) Average chain length as a function of the density for all studied temperatures. (a) Lines are the Wertheim theory predictions: dashed lines assume $g_{HS}=1$ [Eq. (9) for △], while full lines are based on the full radial dependence of g_{HS} [Eq. (8) for △]. (b) Scaled representation of L vs $2\rho\Delta$. Symbols are simulation data. The line is the function $L(x) = (1+\sqrt{1+2x})/2$ [see Eq. (16)].

of the Wertheim theory, we report a comparison between simulations and theory for the density dependence of the extent of polymerization Φ (Fig. 3) and for the energy per particle (Fig. 11). Both figures clearly show an excellent agreement between the simulated and the predicted ρ dependence of Φ and E at all T investigated.

As a test of the validity of the approach of the polymerizing system as an ideal gas of equilibrium chains, we compare the monomer activity z and the monomer density ρ_1 in Fig. 12. The activity of a cluster of size l coincides with ρ_l, which is consistent with ideal gas scaling. In particular, the activity of the single particle (the input in the MC grand-canonical simulation) can be compared with the resulting density of monomers ρ_1. Data in Fig. 12 show that the ideal gas law is well obeyed at low T and ρ, confirming that in the investigated range, the system can be visualized as an ideal gas mixture of chains of different lengths, distributed according to Eq. (14).

The existence of a large T-ρ window where an ideal mixture of chains provides a satisfactory representation of the system suggests that in this window, correlations between different chains can be neglected. In this limit, the structure of the system should be provided by the structure of a single chain, weighted by the appropriate chain length distribution. Specifically, we have
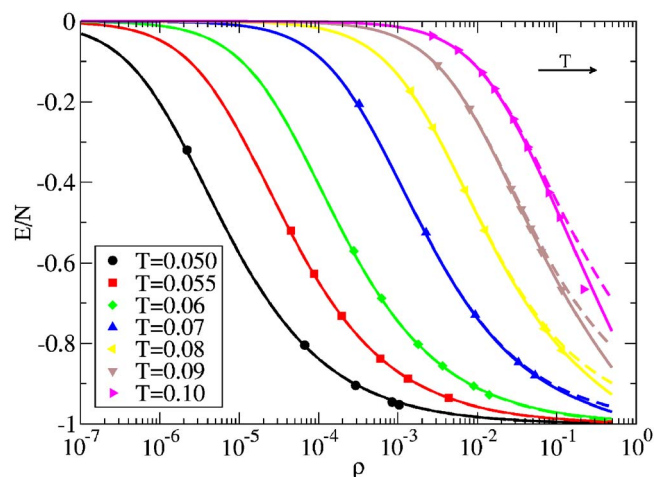

FIG. 11. (Color online) Energy per particle in unit of u_0 as a function of the density for all studied temperatures. Symbols are simulation data while lines are the Wertheim theory predictions: dashed lines assume $g_{HS}=1$ [Eq. (9) for △], while full lines are based on the full radial dependence of g_{HS} [Eq. (8) for △].

$$S(q) \equiv \left\langle \frac{1}{N} \sum_{i,j} e^{-i\mathbf{q}\cdot(\mathbf{r}_i-\mathbf{r}_j)} \right\rangle, \qquad (29)$$

where r_i is the coordinate of particle i, the sum runs over all N particles in the system, and the average $\langle\cdots\rangle$ is over equilibrium configurations. In the ideal gas limit, correlations between different chains can be neglected and $S(q)$ can be formally written as

$$S(q) = \frac{\sum_{l=1}^{\infty} \rho_l l S_l(q)}{\sum_{l=1}^{\infty} \rho_l l}, \qquad (30)$$

where $S_l(q)$ is the structure factor (form factor) of a chain of length l,

$$S_l(q) = \frac{1}{l} \left\langle \sum_{i,j=1}^{l} e^{-i\mathbf{q}\cdot(\mathbf{r}_i-\mathbf{r}_j)} \right\rangle. \qquad (31)$$

Since the persistence length of the chains is $\approx 10-20$ particles (see Fig. 7), one can assume, as a first approximation,
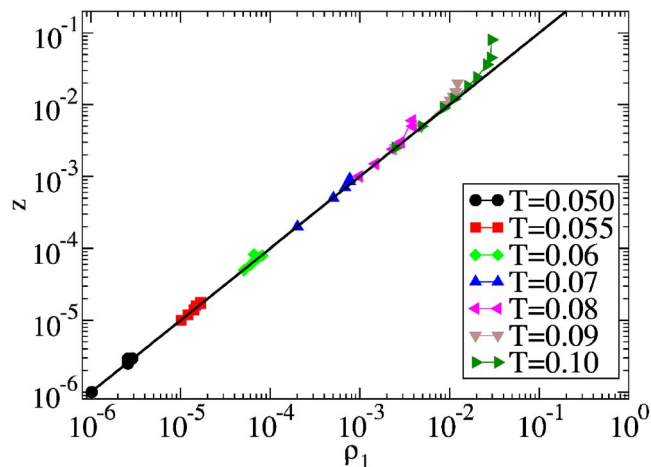

FIG. 12. (Color online) Relation between the activity z and the monomer density ρ_1 for all investigated temperatures. Line indicates the ideal gas law $z=\rho_1$.
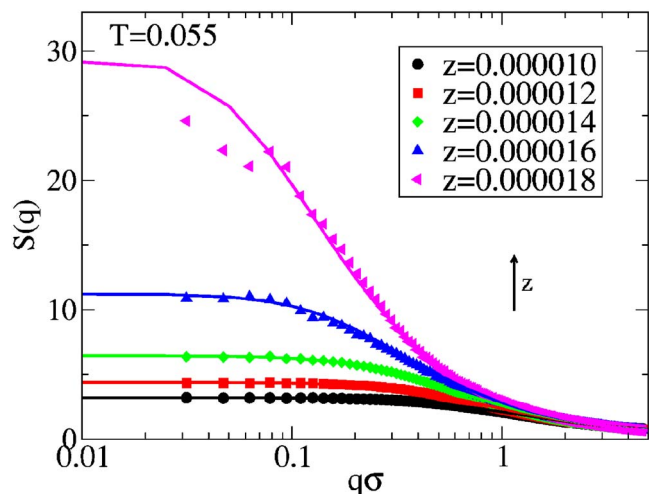
FIG. 13. (Color online) Comparison of the structure factor calculated from the simulated configurations and from Eqs. (30)–(32) at $T=0.055$ for different values of the activity.

that in the investigated T-ρ region chains are linear. When this is the case, averaging over all possible orientations of the chain gives

$$S_l(q) = 1 + \frac{1}{l} \sum_{j=1}^{l-1} 2(l-j) \frac{\sin(jq\sigma)}{jq\sigma}. \tag{32}$$

The small q expansion of $S_l(q)$ is

$$S_l(q) \approx l - \frac{l(l^2-1)}{36}(q\sigma)^2. \tag{33}$$

Correspondingly, $S(q)$ behaves at small q as

$$S(q) \approx \frac{\langle l^2 \rangle}{\langle l \rangle}\left[1 - \frac{q^2\sigma^2}{36}\left(\frac{\langle l^4 \rangle - \langle l^2 \rangle}{\langle l^2 \rangle}\right)\right], \tag{34}$$

where $\langle l^m \rangle \equiv \Sigma_l l^m \rho_l$ denotes the m moment of the cluster size distribution ρ_l. Figure 13 shows a comparison between the $S(q)$ calculated in the simulation and the theoretical $S(q)$ evaluated according to Eqs. (30) and (32) at a low T, where the ideal gas approximation is valid. Deviations are only observed at the highest density, suggesting that the ideal gas of chains is a good representation of the structure of the system, in agreement with the equivalence between activity and monomer density shown in Fig. 12. This observation is particularly relevant since it suggests that (in the appropriate T-ρ window) also a description of the dynamics of the model based on the assumption of independent chains can be attempted.

VII. CONCLUSIONS

In our pursuit of a fully predictive molecularly based theory of self-assembly in terms of molecular parameters and liquid state correlation functions, we have considered a direct comparison of a liquid in which fluid particles have sticky spots on their polar regions to the predictions of the Wertheim theory for the relevant properties governing the self-assembly thermodynamics. In the investigated region of temperatures and densities (which spans the polymerization

transition region), the predictions of the Wertheim theory describe simulation data remarkably well (without the use of any free parameters in these comparisons).

On passing, we stress that we have not investigated state points with $\rho > 0.1$, where interactions between chains start to play a role. A transition from an isotropic to a nematic phase is indeed expected to take place on increasing density.[28,29] The approach to this transition will mark the boundary where the Wertheim theory breaks down. We plan to address this issue in a future work, despite the large computational times involved.

The reported successful comparison means that we can be confident in pursuing more complicated types of self-assembly based on the foundation of the Wertheim theory. For example, it is possible to extend the Wertheim theory analysis in a direct way to describe the self-assembly of branched chains having multifunctional rather than dipolar symmetry interactions as in the present paper and to compare these results in a parameter-free fashion to corresponding MC simulations for these multifunctional interaction particles.[57] A recent work has shown that the Wertheim theory describes the critical properties of these mutifunctional interaction particles rather well.[58] According to this recent study, liquid phases of vanishing density can be generated once small fractions of polyfunctional particles are added to chain-forming models like the one studied here. With the new generation of nonspherical sticky colloids, it should be possible to realize "empty liquids"[58] and observe equilibrium gelation,[44,59,60] i.e., approach dynamical arrest under equilibrium conditions.

The Wertheim theory has also been applied successfully to the description of molecular associating liquids[61–63] and to the thermodynamics of hard-sphere polymer chains with short-range attractive interactions.[64,65] Thus, the theory could be adapted to describe mutually associating polymers and the formation of thermally reversible gels in these fluids upon cooling.

In summary, the Wertheim theory provides a promising framework for treating the thermodynamics of a wide range of self-assembling systems. The development of this theory and its validation by simulation and measurement should provide valuable tools in the practical development of self-assembly as a practical means of synthetic manufacturing. This theory also offers the prospect of improving the existing equilibrium association theories that are largely based on a lattice fluid model framework. This could allow progress to be made more rapidly since off-lattice computation often offers computational advantages and because many problems such as chemically initiated chain branching[66] and thermally activated assembly processes have already been considered by a lattice model of associating fluids.[48,67]

The problem of estimating the entropy of association ΔS_b in real self-assembling molecular and particle systems in solution is a difficult problem that has been addressed by many authors previously (Ref. 68 and references therein). It would clearly be interesting to extend the present work to determine how well the Wertheim theory could predict entropies of association for self-assembly processes that occur in a solvent rather than in the gas phase. The most interesting

solvent in this connection, water, is a particular challenge since water itself can be considered an associating fluid, so that we are confronted with the problem of how the water association couples to the particle self-assembly. The problem of understanding the common tendency of particle self-assembly in aqueous solutions to occur upon heating requires particular investigation. In the future, we look forward to exploring these more complex mixtures of associating fluids, which are so prevalent in real biological systems and in a materials processing context.

As a final comment, we note that numerical work on this class of simple models (playing with the particle interaction symmetries) can help in understanding more complicated ordered structures (for example, sheetlike, nanotube, and closed nanoshell structures), as recently found when particles have multipole interaction potentials.[7,8,10,12] We also note that the results discussed here apply to the growing field of functionalized colloidal particles, colloidal particles with specifically designed shapes and interaction sites.[1–5,69]

ACKNOWLEDGMENTS

[1] V. N. Manoharan, M. T. Elsesser, and D. J. Pine, Science **301**, 483 (2003).

[2] C. A. Mirkin, R. L. Letsinger, R. C. Mucic, and J. J. Storhoff, Nature (London) **382**, 607 (1996).

[3] Y.-S. Cho, G.-R. Yi, J.-M. Lim, S.-H. Kim, V. N. Manoharan, D. J. Pine, and S.-M. Yang, J. Am. Chem. Soc. **127**, 15968 (2005).

[4] G. Yi, V. N. Manoharan, E. Michel, M. T. Elsesser, S. Yang, and D. J. Pine, Adv. Mater. (Weinheim, Ger.) **16**, 1204 (2004).

[5] Y.-S. Cho, G.-R. Yi, S.-H. Kim, D. J. Pine, and S.-M. Yang, Chem. Mater. **17**, 5006 (2005).

[6] F. W. Starr, J. F. Douglas, and S. C. Glotzer, J. Chem. Phys. **119**, 1777 (2003).

[7] S. C. Glotzer, Science **306**, 419 (2004).

[8] S. C. Glotzer, M. J. Solomon, and N. A. Kotov, AIChE J. **50**, 2978 (2004).

[9] Z. Zhang and S. C. Glotzer, Nano Lett. **4**, 1407 (2004).

[10] J. P. K. Doye, A. A. Louis, I.-C. Lin, L. R. Allen, E. G. Noya, A. W. Wilber, H. C. Kok, and R. Lyus, Phys. Chem. Chem. Phys. **9**, 2197 (2007).

[11] F. W. Starr and F. Sciortino, J. Phys.: Condens. Matter **18**, L347 (2006); Langmuir **23**(11), 5896 (2007).

[12] V. Workum and J. F. Douglas, Phys. Rev. E **73**, 031502 (2006).

[13] S. I. Stupp, S. Son, H. C. Lin, and L. S. Li, Science **259**, 59 (1993).

[14] H. Fraenkel-Conrat and R. C. Williams, Proc. Natl. Acad. Sci. U.S.A. **41**, 690 (1955).

[15] P. Buttler, J. Gen. Virol. **65**, 253 (1984).

[16] S. C. Greer, J. Phys. Chem. B **102**, 5413 (1988).

[17] S. C. Greer, Adv. Chem. Phys. **94**, 261 (1996).

[18] S. C. Greer, Annu. Rev. Phys. Chem. **53**, 173 (2002).

[19] I. G. Economou and M. D. Donohue, AIChE J. **37**, 1875 (1991).

[20] G. Jackson, W. G. Chapman, and K. Gubbins, Mol. Phys. **65**, 1 (1988).

[21] N. A. Busch, M. S. Wertheim, and M. L. Yarmush, J. Chem. Phys. **104**, 3962 (1996).

[22] E. A. Müller and K. E. Gubbins, Ind. Eng. Chem. Res. **34**, 3662 (1995).

[23] V. Talanquer and D. W. Oxtoby, J. Chem. Phys. **112**, 851 (2000).

[24] N. A. Busch, M. S. Wertheim, Y. C. Chiew, and M. L. Yarmush, J. Chem. Phys. **101**, 3147 (1994).

[25] Y. Rouault and A. Milchev, Phys. Rev. E **51**, 5905 (1995).

[26] J. P. Wittmer, A. Milchev, and M. E. Cates, J. Chem. Phys. **109**, 834 (1998).

[27] K. V. Workum and J. F. Douglas, Phys. Rev. E **71**, 031502 (2005).

[28] J. T. Kindt, J. Phys. Chem. B **106**, 8223 (2002).

[29] X. Lü and J. T. Kindt, J. Chem. Phys. **120**, 10328 (2004).

[30] J. Stambaugh, K. V. Workum, J. F. Douglas, and W. Losert, Phys. Rev. E **72**, 031301 (2005).

[31] J. Dudowicz, K. F. Freed, and J. F. Douglas, Phys. Rev. Lett. **92**, 045502 (2004).

[32] M. Wertheim, J. Stat. Phys. **35**, 19 (1984).

[33] M. Wertheim, J. Stat. Phys. **35**, 35 (1984).

[34] M. Wertheim, J. Stat. Phys. **42**, 459 (1986).

[35] J. P. Hausen and I. R. McDonald, *Theory of Simple Liquids*, 3rd ed. (Academic, New York, 2006).

[36] G. Jackson, W. G. Chapman, and K. E. Gubbins, Mol. Phys. **65**, 1 (1988).

[37] M. Wertheim, J. Chem. Phys. **85**, 2929 (1986).

[38] R. P. Sear, Curr. Opin. Colloid Interface Sci. **11**, 35 (2006).

[39] I. Nezbeda and G. Iglesia-Silva, Mol. Phys. **69**, 767 (1990).

[40] N. F. Carnahan and K. E. Starling, J. Chem. Phys. **51**, 635 (1969).

[41] T. L. Hill, *An Introduction to Statistical Thermodynamics* (Dover, New York, 1987).

[42] A. Coniglio and W. Klein, J. Phys. A **13**, 2775 (1980).

[43] M. E. Cates and S. J. Candau, J. Phys.: Condens. Matter **2**, 6869 (1990).

[44] E. Zaccarelli, S. V. Buldyrev, E. L. Nave, A. J. Moreno, I. Saika-Voivod, F. Sciortino, and P. Tartaglia, Phys. Rev. Lett. **94**, 218301 (2005).

[45] E. Zaccarelli, I. Saika-Voivod, S. V. Buldyrev, A. J. Moreno, P. Tartaglia, and F. Sciortino, J. Chem. Phys. **124**, 124908 (2006).

[46] A. J. Moreno, S. V. Buldyrev, E. La Nave, I. Saika-Voivod, F. Sciortino, P. Tartaglia, and E. Zaccarelli, Phys. Rev. Lett. **95**, 157802 (2005).

[47] J. Dudowicz, K. F. Freed, and J. F. Douglas, J. Chem. Phys. **111**, 7116 (1999).

[48] J. Dudowicz, K. F. Freed, and J. F. Douglas, J. Chem. Phys. **119**, 12645 (2003).

[49] S. J. Kennedy and J. C. Wheeler, J. Chem. Phys. **78**, 953 (1983).

[50] R. Jones, *Soft Condensed Matter* (Oxford University Press, New York, 2002).

[51] J. F. Douglas, J. Dudowicz, and K. F. Freed, J. Chem. Phys. **125**, 4907 (2006).

[52] R. P. Sear, Phys. Rev. Lett. **76**, 2310 (1996).

[53] B. Smith and D. Frenkel, *Understanding Molecular Simulations* (Academic, New York, 1996).

[54] J. C. LeGuillou and J. Zinn-Justin, J. Phys. (France) **48**, 19 (1987).

[55] J. F. Douglas, T. Ishinabe, A. M. Nemirovsky, and K. F. Freed, J. Phys. A **26**, 1835 (1993).

[56] P. J. Flory, *Principles of Polymer Chemistry* (Cornell University Press, Ithaca, 1953).

[57] E. Bianchi *et al.* (unpublished).

[58] E. Bianchi, J. Largo, P. Tartaglia, E. Zaccarelli, and F. Sciortino, Phys. Rev. Lett. **97**, 168301 (2006).

[59] F. Sciortino, S. Buldyrev, C. De Michele, N. Ghofraniha, E. La Nave, A. Moreno, S. Mossa, P. Tartaglia, and E. Zaccarelli, Comput. Phys. Commun. **169**, 166 (2005).

[60] S. Sastry, E. L. Nave, and F. Sciortino, J. Stat. Mech.: Theory Exp. **2006**, 12010.

[61] J. Kolafa and I. Nezbeda, Mol. Phys. **61**, 161 (1987).

[62] C. Vega and P. A. Monson, J. Chem. Phys. **109**, 9938 (1998).

[63] C. De Michele, S. Gabrielli, P. Tartaglia, and F. Sciortino, J. Phys. Chem. B **110**, 8064 (2006).

[64] C. Vega and L. G. MacDowell, Mol. Phys. **98**, 1295 (2000).

[65] G. Villegas, A. Galindo, P. J. Whitehead, S. J. Mills, G. Jackson, and A. N. Burges, J. Chem. Phys. **106**, 4168 (1997).

[66] F. Tanaka and W. H. Stockmayer, Macromolecules **27**, 3943 (1994).

[67] J. Dudowicz, K. F. Freed, and J. F. Douglas, J. Chem. Phys. **113**, 434 (2000).

[68] M. Mammen, E. I. Shakhnovich, J. M. Deutch, and G. M. Whitesides, J. Org. Chem. **63**, 3821 (1998).

[69] D. Zerrouki, B. Rotenberg, S. Abramson, J. Baudry, C. Goubault, F. Leal-Calderon, D. J. Pine, and J. Bibetteand, Langmuir **22**, 57 (2006).